IEEE Access
Multidisciplinary ⋮ Rapid Review ⋮ Open Access Journal

Received January 6, 2020, accepted February 2, 2020, date of publication February 10, 2020, date of current version February 18, 2020.

Digital Object Identifier 10.1109/ACCESS.2020.2972965

Modeling of Heating and Cooling Energy Needs in Different Types of Smart Buildings

NIKOLAOS A. EFKARPIDIS[1], GEORGIOS C. CHRISTOFORIDIS[2], (Senior Member, IEEE), AND GRIGORIS K. PAPAGIANNIS[3], (Senior Member, IEEE)

[1]Institute of Power Systems, University of Applied Sciences and Arts Northwestern, 5210 Windisch, Switzerland
[2]Electrical and Computer Engineering Department, University of Western Macedonia, 53100 Florina, Greece
[3]School of Electrical and Computer Engineering, Aristotle University of Thessaloniki, 54124 Thessaloniki, Greece

Corresponding author: Grigoris K. Papagiannis (grigoris@eng.auth.gr)

This work was supported by the European Union and National Funds of the participant countries through the Interreg-Balkan MED Programme, under the project 'Enhancing Storage Integration in Buildings with Photovoltaics (PV-ESTIA)', Subsidy Contract BMP1/22/2338/2017.

ABSTRACT Over the last decades, the growing energy consumption of commercial and residential buildings has considerably increased the energy-related carbon dioxide (CO_2) emissions. At EU level, the Energy Performance of Buildings Directive (EPBD) has introduced the transformation of buildings into nearly zero energy buildings (nZEBs) that cover the majority of their low energy demand by on-site renewable energy sources. In this direction, the project PV-ESTIA ''Enhancing storage integration in buildings with Photovoltaics'' aims at developing and validating various optimal energy management strategies in buildings equipped with Photovoltaics (PV) and storage systems. One of the main requirements for the application of the developed strategies is the accurate computation of energy consumption, and particularly, of heating and cooling energy needs. In this paper, a simple and accurate model based on the ''grey-box'' concept is proposed for the computation of hourly thermal energy needs in different types of premises by using the standard ISO 52016-1:2017. The method's performance is evaluated by comparing the results with those of other simulation programs for ten European cities with climatic variations. It is concluded that the proposed model presents high accuracy on the computation of the operative temperature, since it considers the air temperature, as well as the temperatures and the areas of the internal surfaces. Finally, any deviations with the other simulation tools are due to differences in the internal air temperature, weather data, as well as the approaches of ventilation and shading effects.

INDEX TERMS Cooling, energy balance, grey-box, heating, temperature setpoint, U-values.

I. INTRODUCTION

Nowadays, the reduction of energy consumption and the associated greenhouse gas emissions has obtained growing attention in every sector of the economy. In particular, the sectors of buildings and construction are substantial consumers of energy, since they comprise 36% of the global energy usage and 39% of the energy-related carbon dioxide (CO2) emissions [1]. Concerning the global sectors of residential and commercial buildings, it has been calculated that they comprise 20% of the total energy consumption worldwide [2]. Besides that, it is also predicted that the global energy use of the residential sector will increase by around 2.1% per year, from 2012 to 2040 [2]. At the European Union (EU) level, Ref. [3] also predicts that the increasing trend of the energy consumption at the residential sector is expected to result in 50% rise from 1995 to 2050 taking into account the energy use of 1995 as reference. Consequently, a set of strategies and policies shall be established for the residential properties with respect to the future decrease of the energy consumption.

A growing number of policy commitments and strategies have already been observed in terms of activities at local, regional, national and global levels. In the last two decades, several policies and measures have been adopted in EU so as to reduce the energy consumption in the residential sector. At EU level, the measures regard the eco-design and the energy labelling [4], [5], as well as the energy performance and energy efficiency of buildings [6], [7]. At national level, the respective measures comprise various activities, such as provision of subsidies, information campaigns and energy supplier obligations [8]. To this direction,

The associate editor coordinating the review of this manuscript and approving it for publication was Guangya Yang.

EU aims at reducing the greenhouse gas emissions caused by the building sector up to 80-95% by 2050 compared to 1990 levels, as clarified in the Energy Performance of Buildings Directive (EPBD) [9]. Under the EPBD, the EU member states (MSs) shall implement various measures at the national level, such as the Energy Performance Certificates that are issued when buildings are sold or rented. Besides that, the concept of nearly zero energy buildings (nZEBs) has already been introduced in the EPBD of 2010, while the new constructions shall follow this concept by the end of 2010 [10]. In addition, the directive has introduced a methodology that regards cost-optimal Minimum Energy Performance Requirements (MEPs) for new buildings, major renovations of existing buildings, and replacement of retrofit of building elements. Hence, the MSs have to implement measures and other instruments, such as national financial incentives to improve the energy efficiency of their national building stock and to fulfil the requirements of Article 9 of EPBD [10].

Concerning the move towards the increasing implementation of nZEBs, the project PV-ESTIA, ''Enhancing storage integration in buildings with Photovoltaics'' is being carried out in the frame of INTERREG Balkan-Mediterranean 2014-2020. The main goals of this project are both the development and validation of optimal energy management strategies for buildings equipped with Photovoltaics (PV) and storage systems. In particular, the optimal sizing of PV and storage systems taking into account both the electrical and thermal needs of the buildings are of main concern. Besides that, the maximization of self-consumption and the increase of self-sufficiency should always take into account the needs of the distribution network.

A plethora of modelling techniques have been reported extensively in the literature for the calculation of thermal heating and cooling demand in buildings and they can be classified into two categories: physical-based, also known as ''white-box'' models, and data-driven which can be further categorized into ''black-box'' models based on analysis of measured time series, and ''grey-box'' or hybrid models as combination of physical and data-driven approaches. All of the above terminologies differentiate the models based on the capability to describe physical phenomena and on their dependence on data. These three categories are presented in the following subsections.

A. WHITE-BOX TECHNIQUES

The physical-based techniques are based on physical parameters and require a relatively large amount of building knowledge for practical implementations. The fundamental principles of physical-based approches are normally based on the theory of heat transfer and thermodynamics and hence, the methods are based on static and dynamic models, linear and nonlinear equations, as well as differentiable, continuous or non-continuous formulations. The complexity of physical-based modeling depends mainly on the chosen precision levels of the known phenomena associated with the building system to be modeled.

A wide variety of building energy simulation programs based on physical-based techniques, have been developed, enhanced and used for the calculation of thermal energy needs in buildings [11]. The simulation tools most commonly used among the scientific community, are EnergyPlus [12], ESP-r [13], DOE-2 [14] and TRNSYS [15] and can ensure highly accurate results.

In the literature, physical-based techniques mainly use numerical models based on finite element, finite difference and finite volume approaches for the simulation of thermal energy demand in various buildings [16]–[23]. In [16], the author developed a finite-difference method to improve the conduction heat transfer through walls when implementing it in TRNSYS. In addition, an explicit finite-difference method coupled with an enthalpy method to model the thermal behaviour of walls with Phase Change Materials (PCM). Ref. [17] presents a three-dimensional, finite-element, heat-transfer methodology to analyze ground-coupled heat transfer from buildings and the results are compared with the simple ground-coupled heat transfer models applied in commercial simulation tools. Authors in [18] present a dynamic thermal model based on TRNSYS for a building with an integrated ventilated PV façade solar air collector system. A finite difference method is used for the dynamic PV façade thermal model, while heat transfer modelling for the other surfaces of the building is implemented in TRNSYS. In [19], an estimation model was developed for the heating and cooling demand of a residential building with a different envelope design using the finite element method. Authors in [20] developed a dynamic model for the thermal transient analysis of typical single-zone building considering solar irradation and internal radiation. The dynamic behaviour of the indoor temperature is simulated by a finite element model with a lumped approach using a state-space representation developed in MATLAB/Simulink. In [21], the simplified analytical model considers the radiative heat on the inner surface of external envelopes for improving the accuracy of the ''air-to-air'' conduction method. The main goal of the model is to evaluate the impact of inner radiant heat effect on cooling load. Ref. [22] presents a simplified building simulation tool to evaluate energy demand and thermal indoor environment in the early stages of building design. The model is based on limited input data with regards to building design, HVAC systems and control strategies. Hourly values for energy demand and indoor temperature are computed with respect to hourly weather data. Authors in [23] analyze different levels of model complexity, from commercial building energy simulation tools to low order calibrated thermal network models. Experimental data from a residential building in Germany were collected and used to validate two detailed white-box models and a simplified white-box model.

White-box techniques are not practical for large buildings due to: (i) the high computational time required especially for the simulation of hourly thermal energy needs on an annual

basis, (ii) their practical application only for simple buildings due to the difficulty to calibrate the model parameters for buildings with limited sensor information, and (iii) the considerably high amount of building information required for parameter setting.

B. BLACK-BOX TECHNIQUES

As for the black-box models, the parameters can generally be adjusted automatically on the contrary to white-box models where calibration is required. Regarding the internal structure of black-box models, the formulations can be static or dynamic, linear or nonlinear, in the same manner to physical-based techniques. The techniques based on black-box models can be classified into two general types: (a) statistical methods, and (b) supervised machine learning techniques. The former methods are usually related to multiple linear regression models [24]–[27]. Albeit statistical methods are relative straightforward to implement, they can only capture linear relationships among building variables. Since building operations are typically complicated nonlinear, the resulting accuracy of statistical methods can be inadequate. Therefore, supervised machine learning algorithms are mostly applied and the most commonly used methods include support vector machines (SVMs) [28]–[31] and artificial neural networks (ANNs) [31]–[35].

In [24], the sensible cooling load procedure is based on linear regression to find relationships between design conditions, building characteristics, and peak cooling load predicted by residential heat balance. This eliminates the need for semi-empirical adjustments, such as averaging, that have been used in the development of other techniques. Ref. [25] developed and validated metamodels of heating and cooling energy needs for single family houses in six Moroccan climate zones. These metamodels are based on a regression approach with a set of dynamic simulations of the building behaviour. In [26], EnergyPlus is used within a Monte Carlo framework to develop a multivariate linear regression model based on 27 building parameters relevant to the early design stages. Besides that, standardized regression coefficients are presented to quantify the sensitivity of heating, cooling and total energy loads to building design parameters across four different climate zones. Authors in [27] developed regression models that predict office building annual heating, cooling and auxiliary energy requirements for different HVAC systems as a function of office building heating and cooling demands. A large number of building parameters were considered such as built forms, fabrics, glazing levels and orientation leading to 23'040 possible scenarios that were created and simulated through EnergyPlus.

Ref. [28] proposes a prediction model for building energy consumption using SVM technique. The selection of the relevant data to train the SVM model is based on dynamic time warping. Furthermore, a pseudo-dynamic model is applied to encompass the thermal inertia of the building, since it considers information of transition of energy consumption effects and occupancy profile. In [29], short-term multistep-ahead predictive models of heat demand for consumers connected to district heating system are developed using SVMs with Firefly Algorithm (FFA), which is used to optimize SVM parameters. Short-term multi-step ahead predictive models of heat demand of consumers connected to a district heating system are also developed in [30]. The models are developed using the novel method based on SVM coupled with a discrete wavelet transform.

Except the SVM technique, ANNs have largely been applied for the calculation of thermal energy demand in buildings. In [31], traditional back propagation neural network (BPNN), the radial basis function neural network (RBFNN), general regression neural network (GRNN) and SVM techniques are presented for the prediction of hourly cooling demand in a building. Authors in [32] developed an ANN-based advanced thermal control method that consists of a thermal control logic framework with four thermal control logics therein, including two predictive and adaptive logics using ANN models, and a system hardware framework. Ref. [33] developed a surrogate method based on ANN model to speed up the thermal comfort prediction for any member of a building category. The ANN model is generated under MATLAB environment using the data obtained from EnergyPlus simulations for linear-type social housing multi-family buildings in southern Spain. Ref. [34] presents a simulation-based ANN model to characterize building behaviour and in combination with a multiobjective Genetic Algorithm (NSGA-II) for the optimization of thermal comfort and energy consumption in a residential house. In [35], the developed model optimizes the passive design of newly-built residential buildings in China for improving thermal comfort while reducing energy demand of the building. The optimization approach includes: (i) the multi-objective optimization, (ii) sensitivity analysis for reducing the dimensions of input variables, and (iii) the NSGA-II coupled with the ANN.

The main disadvantage of black-box models is their implicit relationship with the physical fundamental principles, especially when there are limited inputs from the building system. Besides that, the black-box models also have limited flexibility, since any change required to describe a slightly difference in physical nature of the model might lead to considerable modifications of the rules or bulk parameters.

C. GREY-BOX TECHNIQUES

The drawbacks of the black-box models could be faced with the use of the grey-box or hybrid models which are more generic, since they can be adapted to model variations in a design. The grey-box models are mixed or transitional forms of white-box and black-box models. The parameters of grey-box models are empirical with a physical significance and can be defined with respect to measured data of a real system. Hybrid models can be developed for the individual components of a system or for a larger complex system. One of the most commonly used grey-box techniques is the representation of the thermal network of a building with a

lumped approach of capacitances and resistances, where the definition of parameters is also based on measured data of a real system.

In [36], a time-series cooling load model deduced from a simplified resistance-capacitance (RC) model approximates the building envelope and internal mass. The performance of the method is tested on a thermal zone in an office building, defined in EnergyPlus as a single zone with an ideal HVAC system. Ref. [37] also presents RC models based on prior physical knowledge and data-driven modelling. The models facilitate insight into various hidden information about the physical properties of the building, such as thermal conductivity, heat capacity, heat capacity of different parts and window area. Authors in [38] propose a simplified thermal network model, where the model parameters of the building envelope are determined using available physical details and the building internal mass is presented with a thermal network structure of 2R2C model. Ref. [39] developed a building model based on a 4R2C approach to simulate the heating load and indoor temperature. In [40], the proposed 7R5C model can accurately calculate thermal demand of a building. The model is combined with weather prediction models operated by a model predictive controller to forecast indoor temeratures for specified rates of supplied energy.

Other grey-box models are based on combinations of RC models for various elements of the building envelope. In [41], the proposed model of heating floor connects a water loop model (1R2C) with two wall models (3R4C). Ref. [42] established second-order simplified formulations for 3TC and 2TC buildings thermal models with straightforward modifications which can improve their accuracy without compromising their simplicity or speed. Authors in [43], [44] propose a grey-box model for building envelope, where the walls and roofs are represented with 3R2C, while the internal mass, including partitions, furniture, etc., is represented with lumped thermal internal mass of 2R2C. In [45], the simple dynamic model consists of several transient energy balance equations for external walls and internal air according to a lumped-capacitance approach for each of the building envelope elements (walls, floor and roof).

Several references have also applied the ISO EN 13790:2008 standard, which proposes a 5R1C thermal model for the calculation of hourly heating and cooling energy demand of buildings [46]–[49]. Authors in [46] propose a 5R1C thermal model based on EN ISO 13790:2008 and allows the correct estimation of the user profile with limited and not sufficiently precise input data. In [47], the proposed method is compared to EN 13790:2008 and it differs, since it considers additional physical laws for the conversion of solar short-wave thermal radiation energy admitted into the room into thermal energy. Ref. [48] presents a simplified standalone, building energy standard based on EN 13790:2008 that was developed by Global Sustainability Assessment System (GSAS) to support Qatar's and the MENA region building energy ratings. In [49], the annual heating and cooling energy needs are calculated for residential and commercial buidlings, through EnergyPlus, ISO 13790:2008 and INVERT/EE-Lab - Thermal Module, which models the stock of buildings in a highly disaggregated manner.

Nowadays, the grey-box approaches are mostly preferred over the black-box ones due to the lack of the physical interpretation of the results in the latter models. Finally, the hybrid models can provide smooth solutions based on twice differentiable equations which enhance the robustness of the dynamic optimization compared to the black-box models which are based on global optimization methods.

D. MAIN PAPER CONTRIBUTIONS

As a replacement of the simplified method used in ISO 13790:2008, the ISO 52016-1:2017 standard introduced a new methodology for the assessment of the building energy performance. To the best of the authors' knowledge, a limited number of studies have been carried out for the performance of the standard with respect to the hourly heating and cooling energy needs of buildings [50], [51]. In [50], the quasi-steady procedure of EN ISO 52016-1, which uses the concept of the utilization factors for energy gains and heat transfer, was developed. In particular, a calibration of the summer quasi-steady models was carried out, by means of the results provided by TRNSYS, referring to different configurations of two buildings. However, the authors focused only on the comparison of monthly cooling demands between EN ISO 52016-01 and TRNSYS. Ref. [51] presents a comprehensive analysis of the ISO 52016-1:2017 accuracy with respect to a wide range of building uses, envelope properties, as well as annual and hourly heating/cooling needs. The analysis was performed by comparing the results from the standard with the dynamic simulation in TRNSYS. Nevertheless, the study has not considered the impact of different building locations on the thermal energy needs.

Since the project PV-ESTIA focuses on the development of optimal energy management methods with PV-storage systems for various types of buildings, it is of upmost importance to calculate the hourly heating and cooling energy needs in different European countries. To this direction, this paper develops a simple and accurate method based on ISO 52016-01 for the computation of hourly heating and cooling energy needs in different types of buildings. The method was firstly presented and evaluated for a multi-apartment block in [52]. While in this work, the model is evaluated in two different instances of residential buildings, the robustness of the method ensures its applicability for other types of premises as well. Since the proposed model is considered as one of the modules that comprise the optimal energy management strategies developed in the frame of PV-ESTIA project, it should guarantee high accuracy and simplicity. The performance of the model is evaluated by comparing the results of the proposed model with the results from the European project ENTRANZE [49], where the EnergyPlus, EN 13790:2008 and INVERT/EE-Lab - Thermal Module were utilized.

E. PAPER STRUCTURE

The remainder of this paper is structured as follows. Section II describes the formulations of the thermal energy model utilized for the simulations. Next, the thermal energy calculation procedure is presented in Section III, followed by the inputs and assumptions that are provided in Section IV. The results are presented and interpreted in Section V, while the summary of conclusions is provided in Section VI.

II. THERMAL ENERGY MODELING

The proposed thermal model used for the computation of internal air temperature, as well as of both heating and cooling energy needs in residential premises, on hourly basis for the whole year, is based on the hourly calculation method of EN ISO 52016-01:2017 [53].

Several assumptions are made in the proposed model for simplicity reasons. First, the ventilation and infiltration components are aggregated, and no air handling units are considered for the residential buildings. In addition, a single thermal zone is considered for each building envelope, thus, a common temperature is assumed for the total volume of each investigated building. Besides that, the opaque building elements are considered to be composed of thermally homogeneous layers, while the thermal bridges in the building envelope are omitted.

A. HOURLY METHOD

The hourly heating and cooling energy needs of a building are defined by a set of energy balance equations. First, the internal operative temperature shall be calculated for the definition of the energy needs. The energy balance equations consider the effects of transient heat transfer between the exterior and the interior of the building components, as well as the effect of the thermal mass. In particular, one energy balance equation is considered for the thermal zone of the building, and one energy balance equation for each node of the building elements.

As depicted in Fig. 1, the glazed elements (windows) are modelled with one layer of two nodes, while the opaque building elements (walls, roof and floor) are divided into four layers and five nodes. The numeration of nodes is set from exterior to interior with regards to a convention, thus, the first node corresponds to the closest node to the outer surface of the element, and the last node represents the inner surface of the building component. Concerning the building nodes,

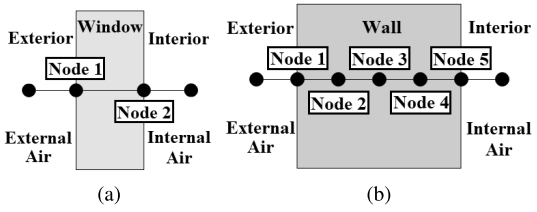

FIGURE 1. Nodal distribution in the building elements: (a) windows, and (b) walls, roof and the floor.

Fig. 2 illustrates an analytical representation of the processes that are considered by the energy balance equations for the nodes of the building elements.

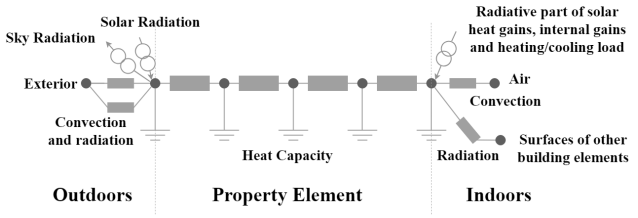

FIGURE 2. Equivalent RC model for the building element energy balances.

The temperatures $\theta_{air,t}$ and $\theta_{ext,t}$ correspond to the internal and external air temperatures, respectively, while the temperature $\theta_{surf,k,t}$ represents the temperature of the last node of each element k. In addition, the internal gains $\Phi_{int,t}$, solar gains $\Phi_{sol,t}$ and thermal loading due to heating or cooling, $\Phi_{HC,t}$ are taken into account. The corresponding convention factors f_{int}, f_{sol} and f_{HC} are equal to 0.40, 0.10 and 0.40, respectively, according to [53].

B. SYSTEM OF LINEAR EQUATIONS

The system of linear equation has the typical form $Ax = B$, where A corresponds to a square matrix with the coefficients of the unknown temperatures $\theta_{i,t}$ (in °C), B is a vector that includes the source terms and boundary conditions, and the x vector represents the unknown temperatures. The linear equations are based on the primary energy balance equation, as follows:

$$\frac{C_i}{\Delta t} \cdot (\theta_{i,t} - \theta_{i,t-1}) = H_{i,t-1} \cdot (\theta_{i+1,t} - \theta_{i,t}) + \Phi_{i,t} \quad (1)$$

where Δt is the hourly timestep (in sec) and C_i, $H_{i,t}$, $\Phi_{i,t}$ represent the thermal capacity (in J/(m^2·K)), conductance (in W/(m^2·K)) and gain (in W) of the building component i at time increment t, respectively. The one-dimensional, unsteady heat conduction equation can be discretized through (1) in an implicit form.

C. THERMAL ZONE LEVEL

The energy balance of the thermal zone considers the heat transfer of each building component with area A_k, the internal air, as well as the thermal inertia and the heat transfer coefficients due to ventilation, $H_{vent,t}$ and infiltration, $H_{infilt,t}$, as depicted in (2), as shown at the bottom of the next page.

The internal thermal capacity of the thermal zone, C_{int} is computed by:

$$C_{int} = k_{int} \cdot A_{use} \quad (3)$$

where k_{int} represents the thermal capacity of air and furniture and is approximately 10'000 J/(m^{2}K) [54]. The useful floor area A_{use} consists of the horizontal area in each building level that is enclosed inside the building envelope and expected to be heated more than 10°C. The conventional internal surface heat transfer coefficient $h_{int,conv,k}$ of each element A_k

depends on the direction of the heat flow, and is equal to 5.00, 2.50 and 0.70 W/(m^2·K) for upwards, horizontal and downwards direction, respectively [53].

The ventilation heat transfer coefficient $H_{vent,t}$ is computed considering the hourly air flow rate, $q_{V,t}$, as follows:

$$H_{vent,t} = \rho_\alpha \cdot c_\alpha \cdot q_{V,t} \tag{4}$$

where ρ_α is the air density at 20°C, which is 1.204 kg/m^2, and c_α is the specific heat of air at constant pressure, which is 1006 J/(kg·K). The $q_{V,t}$ can be considered as equal to 0.5 l/s per m^2 of the useful floor area in case of residential buildings [55]. In the same manner to ventilation, the heat transfer coefficient for infiltration can also be assumed as 0.5 changes per hour (ACH) [56].

The internal heat gains of the thermal zone are computed by:

$$\Phi_{int,t} = F_{occ,t} \cdot q_{occ} + F_{app,t} \cdot q_{app} \tag{5}$$

where the internal gains of occupants, q_{occ} and appliances, q_{app} are given in [55]. For the purposes of this study, the usage factors for occupants, $F_{occ,t}$ and appliances, $F_{app,t}$ in case of residential dwellings can also be determined by [55]. According to [53], the total solar heat gain through glazed elements are calculated, as follows:

$$\Phi_{sol,t} = \sum_{k=1}^{glazings} s_k \cdot g_k \cdot I_{k,t} \cdot A_k \cdot (1 - F_{fr,k}) \tag{6}$$

where the g-values, g_k and the frame area fractions, $F_{fr,k}$ are referred to glazing element k of the building, and $I_{k,t}$ corresponds to the incident solar radiation. The shading factor values s_k can be either constant or variable with respect to a specific shading schedule.

D. BUILDING ELEMENT LEVEL

As already mentioned, the energy balance equations at each building element include one equation for each of the building element nodes, particularly, internal and external surface nodes, as well as the inner nodes. Equation (7), as shown at the bottom of this page, represents the energy balance equation for the internal surface node of each building element.

Concerning the areal heat capacity k_n, we define the class of the building element with regards to its mass distribution. The existence of insulation has impacts on the thermal mass distribution of the opaque elements. On the other hand, the areal heat capacity of the windows is zero, since the thermal mass of glazing components can be neglected.

Regarding the opaque components of the building in contact with the air, each node has a different areal heat capacity with respect to the mass distribution in the component. In particular, the mass distribution is classified into five categories: (a) mass concentrated at the internal side, (b) mass concentrated at the external side, (c) mass divided over interior and exterior, (d) equally distributed mass, and (e) mass concentrated at the inner part of the element, as shown in Table 1. Table 2 displays default values for k_m, as suggested in [53].

TABLE 1. Values of areal heat capacity for Opaque Components in contact with air and ground.

Mass Distribution	Values of k_n	
	Air	Ground
Mass concentrated at internal side	k_5=k_m, k_1=k_2=k_3=k_4=0	k_2=k_{gr}, k_5=k_m k_1=k_3=k_4=0
Mass concentrated at external side	k_1=k_m, k_2=k_3=k_4=k_5=0	k_2=k_{gr}, k_3=k_m, k_1=k_4=k_5=0
Mass divided over interior and exterior	k_1=k_5=$k_m/2$ k_2=k_3=k_4=0	k_1=k_4=0, k_2=k_{gr}, k_3=k_5=$k_m/2$
Equally distributed mass	k_1=k_5=$k_m/8$ k_2=k_3=k_4=0	k_2=k_{gr}, k_3=k_5=$k_m/4$ k_1=0, k_4=$k_m/2$
Mass concentrated inside	k_3=k_m, k_1=k_2=k_4=k_5=0	k_2=k_{gr}, k_4=k_m, k_1=k_3=k_5=0

Regarding the opaque components in contact with the ground, the areal heat capacity for all nodes with respect to the type of mass distribution is also displayed in Table 1. In particular, k_{gr} corresponds to the areal heat capacity of the fixed ground element for a thick ground layer of 0.5 m. Table 3 shows different values of k_{gr} with respect to the type of soil and various cases, according to [57].

$$\left[\frac{C_{int}}{\Delta t} + \sum_{k=1}^{elements}(A_k \cdot h_{int,conv,k}) + H_{vent,t} + H_{infilt,t}\right] \cdot \theta_{air,t} - \sum_{k=1}^{elements}(A_k \cdot h_{int,conv,k} \cdot \theta_{surf,k,t})$$
$$= \frac{C_{int}}{\Delta t} \cdot \theta_{air,t-1} + (H_{vent,t} + +H_{infilt,t}) \cdot \theta_{ext,t} + f_{int} \cdot \Phi_{int,t} + f_{sol} \cdot \Phi_{sol,t} + f_{HC} \cdot \Phi_{HC,t} \tag{2}$$

$$-(h_{n-1} \cdot \theta_{n-1,t}) + \left[\frac{k_n}{\Delta t} + h_{int,conv,k} + h_{int,rad} \cdot \sum_{\substack{j=1 \\ j\neq k}}^{elements}\left(\frac{A_j}{A_{tot}}\right) + h_{n-1}\right] \cdot \theta_{n,t} - (h_{int,conv,k} \cdot \theta_{air,t})$$
$$- \sum_{\substack{j=1 \\ j\neq k}}^{elements}\left(\frac{A_j}{A_{tot}} \cdot h_{int,rad} \cdot \theta_{n,j,t}\right) = \frac{k_n}{\Delta t} \cdot \theta_{n,t-1} + \frac{1}{A_{tot}} \cdot \left[(1 - f_{int}) \cdot \Phi_{int,t} + (1 - f_{sol}) \cdot \Phi_{sol,t} + (1 - f_{HC}) \cdot \Phi_{HC,t}\right] \tag{7}$$

TABLE 2. Values of k_m according to the class of construction.

Class	k_m J/(m^{2}K)	Description of Class
Very light	50000	No mass components other than plastic board and/or wood siding, or similar.
Light	75000	No mass components other than 5-10 cm of lightweight brick or concrete, or similar.
Medium	110000	No mass components other than 10-20 cm of lightweight brick or concrete, or less than 7 cm of solid brick or heavyweight concrete, or similar.
Heavy	175000	7-12 cm of solid brick or heavyweight concrete, or similar.
Very Heavy	250000	>12 cm of solid brick or heavyweight concrete, or similar.

TABLE 3. Areal heat capacity of the fixed ground component and thermal conductivity of ground.

Type of Soil	k_{gr} J/(m^{2}K)	λ_{ground} W/(mK)
Clay or silt	$1.5{\cdot}10^6$	1.5
Sand or gravel	$1.0{\cdot}10^6$	2.0
Homogeneous rock	$1.0{\cdot}10^6$	3.5

On the contrary to the conventional surface heat exchange coefficients, the internal radiative surface coefficient, $h_{int,rad}$ is equal to 5.13 W/(m^2·K), regardless of the heat flow direction [58]. As shown in (8) at the bottom of this page, the total area of the building components A_{tot} is also required.

In the same manner to the areal heat capacity, the conductances h_n between the nodes of the building components depend on their class. As a result, different values are considered for opaque components in contact with the external air and for opaque components in contact with the ground and glazed components.

As for the opaque components in contact with the external air, the conductances between the nodes are provided by:

$$h_1 = h_4 = \frac{6}{R_k}, \quad h_2 = h_3 = \frac{3}{R_k} \tag{9}$$

where R_k represents the thermal resistance of the building component k in (m^2·K)/W. According to [59], the thermal resistance R_k is determined by:

$$R_k = \frac{1}{U_k} - R_{si} - R_{se} \tag{10}$$

where R_{si} and R_{se} are the thermal resistances for the internal and external surfaces, respectively.

Concerning the glazed components, the conductance between the nodes, h_1 is equal to $1/R_k$, where R_k is calculated by (10), and the U-value of the window includes the frame as well.

As for the components in contact with the ground, the conductances between nodes are as follows:

$$h_1 = \frac{2}{R_{ground}}, \quad h_2 = \frac{1}{\left(\frac{R_k}{4} + \frac{R_{ground}}{2}\right)},$$
$$h_3 = \frac{2}{R_k}, \quad h_4 = \frac{4}{R_k} \tag{11}$$

where R_{ground} corresponds to the thermal resistance of 0.5 m of ground, in (m^2·K)/W and is equal to $0.5/\lambda_{ground}$. The thermal conductivity of the ground λ_{ground} depends on the type of soil [57], and is depicted in Table 3. Regarding the elements in contact with the ground, the thermal resistance, R_k, is computed by (10) neglecting R_{se}.

Equation (12), as shown at the bottom of the next page, represents the energy balance equation for the internal nodes of each surface, while the corresponding equation for the node of each external surface is provided in (13), as shown at the bottom of the next page. As for the external surface heat transfer coefficients, the conventional coefficient, $h_{ext,conv}$ and the radiative coefficient, $h_{ext,rad}$ are considered as equal to 20 W/(m^2·K) and 4.14 W/(m^2·K), respectively, according to [58].

Regarding the elements in contact with the ground, the external convective and radiative surface heat transfer coefficients are substituted by the heat transfer with the ground. The heat transfer with the ground is represented by $1/R_{ground,virtual}$, where $R_{ground,virtual}$ corresponds to the thermal resistance of a virtual ground layer. Based on [57], this thermal resistance is computed, as follows:

$$R_{ground,virtual} = \frac{1}{U_k} - R_{si} - R_{floor} - R_{ground} \tag{14}$$

where R_{floor} represents the thermal resistance of the floor.

The solar absorption coefficient, a_{sol} at the external surfaces of the building depends on the surface color, as explained in [53]. A typical value for light, intermediate and dark colors is 0.30, 0.60 and 0.60, respectively. As for the components in contact with the ground and glazed components, this coefficient is equal to zero.

The thermal radiation to the sky, Φ_{sky} is computed by:

$$\Phi_{sky} = F_{sky} \cdot h_{ext,rad} \cdot \Delta\theta_{sky} \tag{15}$$

$$-(h_{n-1} \cdot \theta_{n-1,t}) + \left[\frac{k_n}{\Delta t} + h_{int,conv,k} + h_{int,rad} \cdot \sum_{\substack{j=1 \\ j\neq k}}^{elements} \left(\frac{A_j}{A_{tot}}\right) + h_{n-1}\right] \cdot \theta_{n,t} - (h_{int,conv,k} \cdot \theta_{air,t})$$
$$- \sum_{\substack{j=1 \\ j\neq k}}^{elements} \left(\frac{A_j}{A_{tot}} \cdot h_{int,rad} \cdot \theta_{n,j,t}\right) = \frac{k_n}{\Delta t} \cdot \theta_{n,t-1} + \frac{1}{A_{tot}} \cdot \left[(1 - f_{int}) \cdot \Phi_{int,t} + (1 - f_{sol}) \cdot \Phi_{sol,t} + (1 - f_{HC}) \cdot \Phi_{HC,t}\right] \tag{8}$$

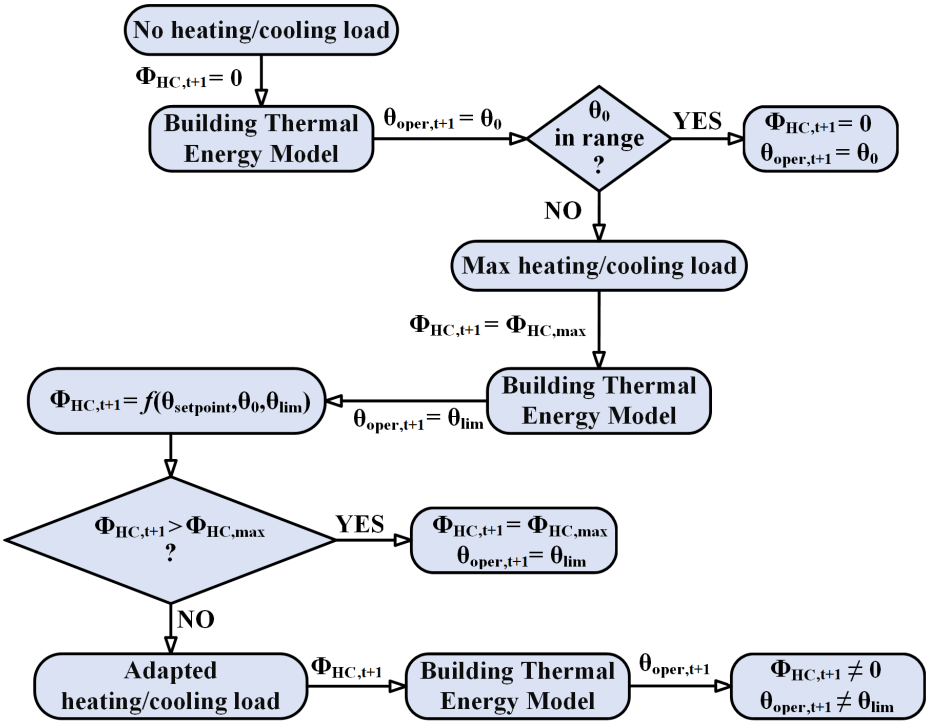

FIGURE 3. Flowchart for the calculation of thermal energy needs for the examined building.

where the view factor from each component to the sky, F_{sky} is 1 for roofs and 0.5 for vertical walls. The average difference between the apparent sky temperature and the air temperature, $\Delta\theta_{sky}$ is 9 K, 11 K and 13 K, in sub-polar, intermediate and tropical zones, respectively [53].

III. THERMAL ENERGY CALCULATION ALGORITHM

The hourly thermal energy consumption depends on the internal air temperature, which depends on the temperatures at the previous time increment and the boundary constraints. The hourly thermal energy needs are indicated by $\Phi_{HC,t}$. At each time increment, the procedure displayed in Fig. 3 is carried out.

First, the internal operative temperature is calculated assuming zero thermal energy demand for the building, therefore, it is considered as operative temperature in free-floating conditions (θ_0). The range of setpoints determines if there is need for heating or cooling the building. If θ_0 remains inside the predefined range, no thermal energy demand exists. The internal air temperature, as well as the temperatures of all the nodes remain constant at the next timestep, therefore, they shall be stored for the following timestep.

When the operative temperature is outside the range, thermal heating or cooling of the building is needed. In this case, the thermal energy demand is set to the maximum available power capacity of the heating or cooling units, $\Phi_{HC,max}$, and the new operative temperature θ_{lim}, which corresponds to the maximum or minimum possible value, is computed. Next, the operative load is provided by:

$$\Phi_{HC,t+1} = \Phi_{HC,max} \cdot \frac{(\theta_{setpoint} - \theta_0)}{(\theta_{lim} - \theta_0)} \tag{16}$$

The operative load is compared with the rated power capacity for heating or cooling $\Phi_{HC,max}$. If the computed load is lower than the rated power capacity, the final load will be the computed one, and the actual operative temperature will be set to the setpoint $\theta_{setpoint}$. Next, the internal air temperature and the temperature of each node will be calculated using the previously computed load and will be stored for the next timestep. If the operative load is higher than the rated power capacity, the final load will be set as the rated power of the thermal unit and the temperatures for the next timestep will be equal to the ones calculated for the maximum available power.

$$-(h_{n-1} \cdot \theta_{n-1,t}) + \left(\frac{k_n}{\Delta t} + h_n + h_{n-1}\right) \cdot \theta_{n,t} - (h_n \cdot \theta_{n+1,t}) = \frac{k_n}{\Delta t} \cdot \theta_{n,t-1} \tag{12}$$

$$\left[\frac{k_n}{\Delta t} + h_{ext,conv} + h_{ext,rad} + h_1\right] \cdot \theta_{1,t} - (h_1 \cdot \theta_{2,t}) = \frac{k_n}{\Delta t} \cdot \theta_{1,t-1} + (h_{ext,conv} + h_{ext,rad}) \cdot \theta_{ext,t} + \alpha_{sol} I_{k,t} - \Phi_{sky} \tag{13}$$

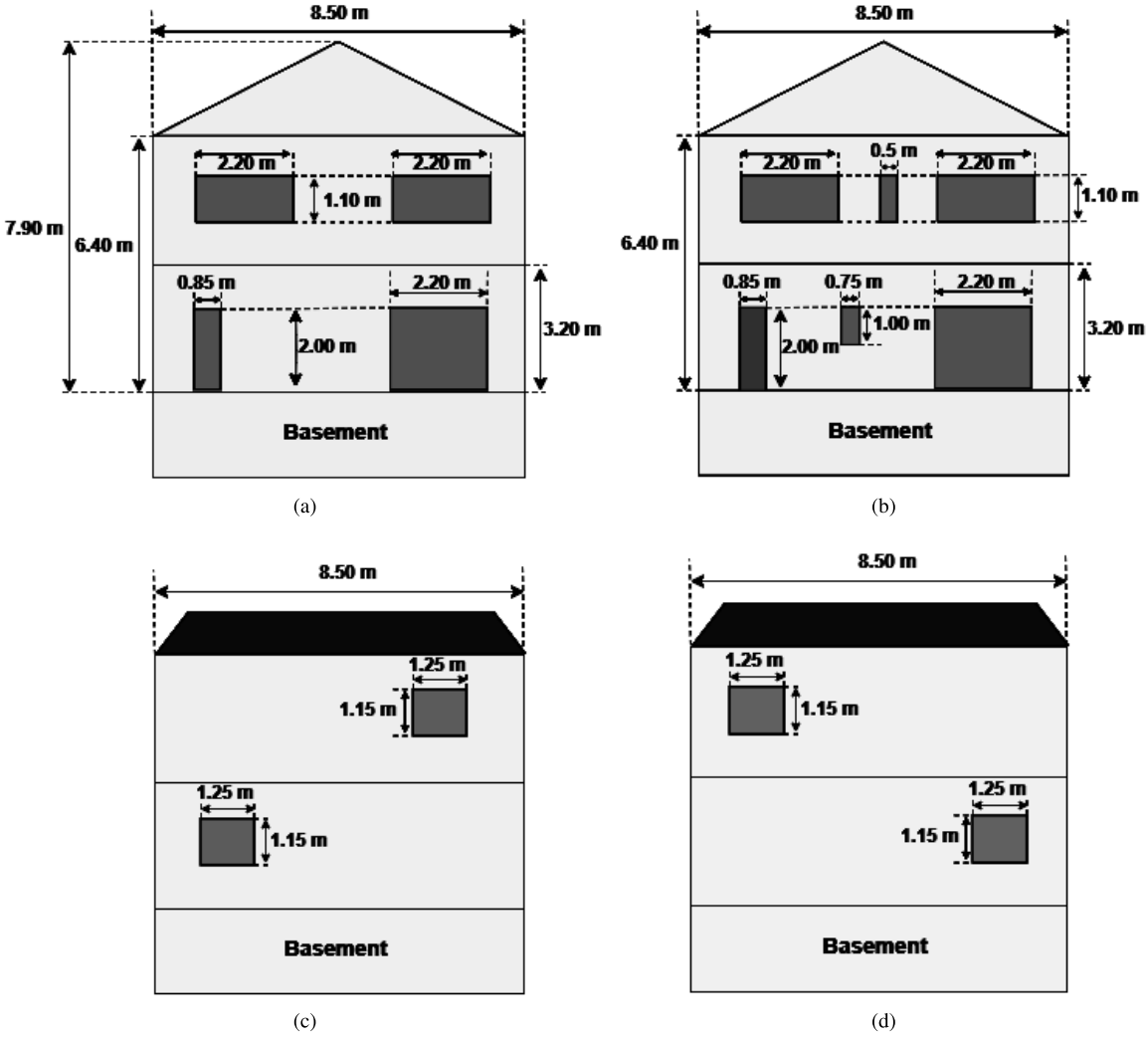

FIGURE 4. Prospects of the investigated single-family house: (a) north facade (b) south facade (c) east facade (d) west facade.

The operative temperature $\theta_{oper,t}$ is computed, as follows:

$$\theta_{oper,t} = \frac{\theta_{air,t} + \theta_{mean,t}}{2} \tag{17}$$

where $\theta_{mean,t}$ corresponds to the mean radiant temperature that is the weighted average of the internal surface temperature of all the building elements:

$$\theta_{mean,t} = \frac{\sum_{k}^{elements}(\theta_{surf,k,t} \cdot A_k)}{\sum_{k}^{elements}(A_k)} \tag{18}$$

For the high accuracy of the model, the appropriate input of the previous node temperatures should be used, therefore, an initialization procedure is carried out by applying the proposed thermal energy calculation algorithm with historical data of one month, such as December, for the sake of consistency.

IV. INPUTS AND ASSUMPTIONS

Two types of residential buildings, as presented in [49], are examined for ten locations in different EU countries: (a) a single-family house, and (b) a multi-apartment block. In particular, the buildings are located in: (i) Seville, Spain (ES), (ii) Madrid, Spain (ES), (iii) Rome, Italy (IT), (iv) Milan, Italy, (v) Bucharest, Romania (RO), (vi) Vienna, Austria (AT), (vii) Paris, France (FR), (viii) Prague, Czech Republic (CZ), (ix) Berlin, Germany (DE) and (x) Elsinki, Finland (FI). The simulations of the proposed model were carried out in MATLAB R2018a.

For both types, a constant infiltration rate of 0.77 ACH is assumed during the year, while a constant ventilation rate of 0.5 l/s per m^2 is considered only at summer nights. The weekly schedules for both occupants and equipment are provided in Appendix A. The temperature setpoints for heating and cooling are considered to be equal to 20°C and 26°C, correspondingly, and are continually applied, as the occupancy factor profile $F_{occ,t}$ considered has non-zero values. Concerning the absorptivity of the walls, intermediate colors were considered for the walls of both buildings. The thermal mass distribution is assumed to be concentrated at the internal side for the roofs and divided over interior and

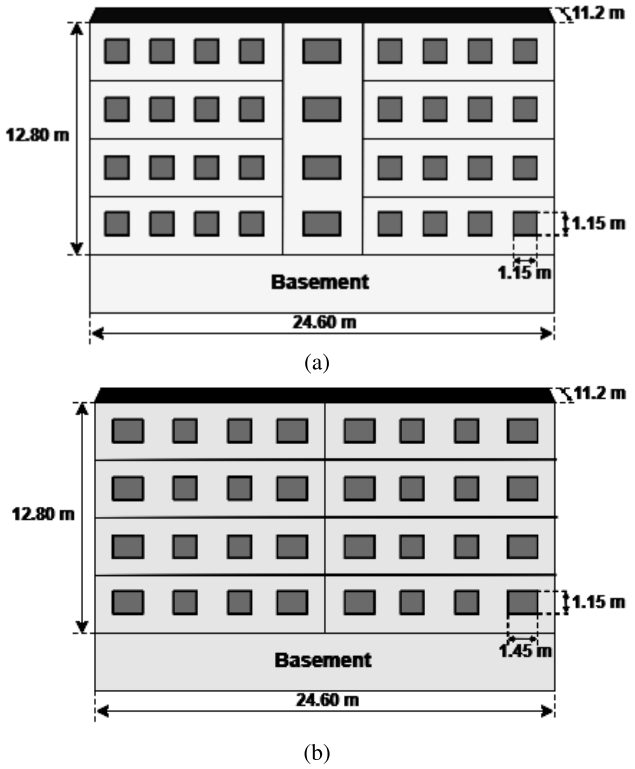

FIGURE 5. Prospects of the investigated multi-apartment block: (a) north facade (b) south facade.

exterior for the insulated walls. In case of insulation absence, the mass is equally distributed on the opaque components. The profiles of hourly external air temperature and solar irradiance in the surfaces of each building during the year using specific coordinates are given by [60]. The main characteristics related to geometry and internal gains are provided by [49], and are described in the next subsections. Despite the various building architectures used in different European areas, the same architecture was considered in all examined countries for each type in order to obtain credible comparison results.

A. SINGLE-FAMILY HOUSE

The building, which is selected as reference for single-family house, consists of an underground level and two floors over level and has a conditioned surface area of about 140 m^2. Fig. 4 displays the prospects of the building, where the dimensions of both opaque and glazing building elements are provided. The main fixed and variable characteristics of the single-family house with respect to the locations of the investigated countries are displayed in Appendix B.

B. MULTI-APARTMENT BLOCK

The multi-apartment block is composed of four floors and a cellar, with conditioned area of about 1000 m^2, as displayed in Fig. 5. The main characteristics (fixed and variable by country) involved in the simulation task are provided in Appendix B.

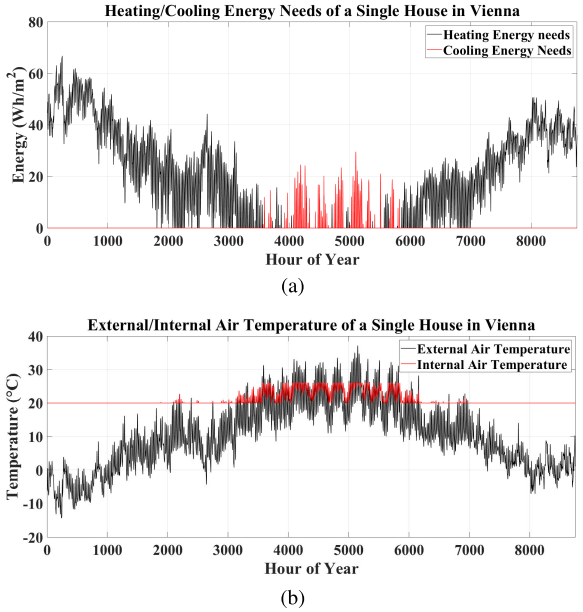

FIGURE 6. For a single-family house in Vienna: (a) the hourly heating and cooling energy needs, and (b) the hourly internal and external air temperatures.

V. RESULTS

A. SINGLE-FAMILY HOUSE

First, the hourly heating and cooling energy needs, as well as temperatures of internal and external air for a single-family house in Vienna are displayed in Fig. 6. As can be observed, the heating and cooling seasons are distinctly divided, while there are short time intervals in spring and autumn with zero thermal energy needs. Besides that, the heating needs show a gradual increase from September to December, with a peak value of about 65 W/m^2 and a gradual decrease from December to May, with a local peak value of about 45 W/m^2 in March. On the other hand, the cooling needs present a non-uniform distribution from May to August with a peak value of around 30 W/m^2.

It is also evident that the internal air temperature of the investigated single-family house remains inside the range [20°C 26°C], as predefined by the heating and cooling setpoints. To be highlighted, the temperature setpoints are set for the whole year, while in practice, the occupants usually deactivate the space heating/cooling when they are absent. Hence, the results are expected to be slightly conservative compared to the real thermal energy needs. It can also be noticed that from March to October there are time intervals when no energy needs for heating and cooling exist, since the internal air temperature remains inside the range [20°C 26°C].

Next, the outcomes of the developed method on annual and monthly basis are compared with the outcomes derived from other simulation tools for various European locations in the frame of the project ENTRANZE [49].

As illustrated in Table 4, the annual heating and cooling needs from the application of ISO 52016-1 model have differences with EnergyPlus, EN13790 and INVERT/

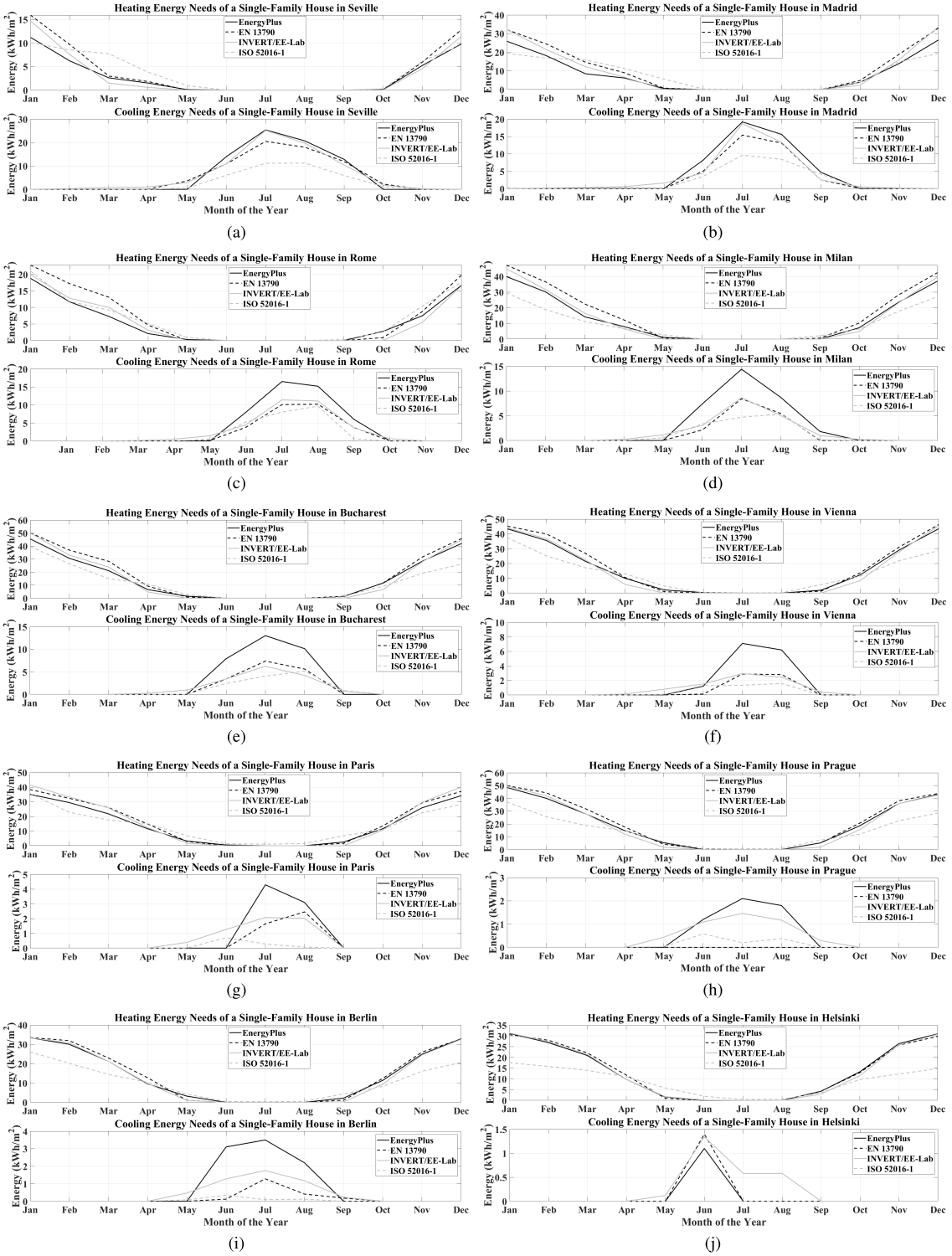

FIGURE 7. Monthly Thermal Energy Needs of a Single-Family House in: (a) Seville, (b) Madrid, (c) Rome, (d) Milan, (e) Bucharest, (f) Vienna, (g) Paris, (h) Prague, (i) Berlin, (j) and Helsinki.

EE-Lab, however, the differences vary on the location of the single-family house. Concerning the annual heating energy needs, the results of ISO 52016-1 have slight variations mainly with EnergyPlus, while the annual cooling energy needs of ISO 52016-1 mostly approximate the results of EN13790 method. Albeit the lowest temperature profile was noticed in Helsinki, the heating demand of the corresponding building was considerably lower compared to the buildings located in Bucharest, Vienna, Paris and Prague. This occurs due to the additional reinforcement of the building construction material which containts insulation, while the other buildings include only the main materials of brick, concrete

TABLE 4. Summary of annual heating and cooling energy needs for the single-family house.

Method [1]	Annual Heating Energy Needs (kWh/m^2)				Annual Cooling Energy Needs (kWh/m^2)			
	A	B	C	D	A	B	C	D
Seville	36.700	24.400	20.300	47.811	72.900	66.900	75.100	35.943
Madrid	103.90	137.48	125.56	107.99	47.700	35.740	42.840	25.891
Rome	67.100	87.090	68.040	79.163	45.800	27.910	34.550	24.018
Milan	160.90	200.05	168.20	122.12	32.400	15.930	19.830	14.067
Bucharest	189.10	215.12	191.65	150.60	31.000	16.470	16.470	12.484
Vienna	199.50	214.95	191.59	165.54	14.500	5.0860	9.0960	4.2388
Paris	176.00	195.80	195.79	170.42	7.4000	4.1090	7.2370	1.0721
Prague	239.40	255.77	230.80	175.10	5.2000	0.0000	4.8170	1.1869
Berlin	168.70	173.83	162.46	125.81	8.9000	1.7500	5.5420	0.6324
Helsinki	165.20	165.65	162.73	107.15	1.2000	1.4600	3.2137	0.0000

[1] A: EnergyPlus, B: EN13790, C:INVERT/EE-Lab, D: ISO52016-1

and plaster. On the contrary, the cooling energy needs are considerably lower than the heating energy needs. Only in Seville, the aforementioned needs have slight difference due to the high temperature profile of the external air.

Fig. 7 depicts the monthly heating and cooling energy needs of a single-family house located in the investigated cities. It is evident that the results from the evaluated models with regards to heating demand have slighter differences compared to the respective results of cooling energy needs. Besides that, it can be noticed that the building located in the most southern investigated city of Seville presents the lowest peak heating needs and the highest peak cooling needs due to the high temperature profile during the year. On the other hand, the buildings located in Bucharest and Helsinki show the highest peak heating needs and the lowest peak cooling needs, respectively. In terms of heating demand, the highest deviations of ISO 52016-01 with the other simulation tools were noticed for the buildings in Prague and Helsinki. Concerning for the cooling demand, the monthly differences of ISO 52016-01 with the other models vary from location to location during the summer period, while the accuracy is considerably high for the other months of the year.

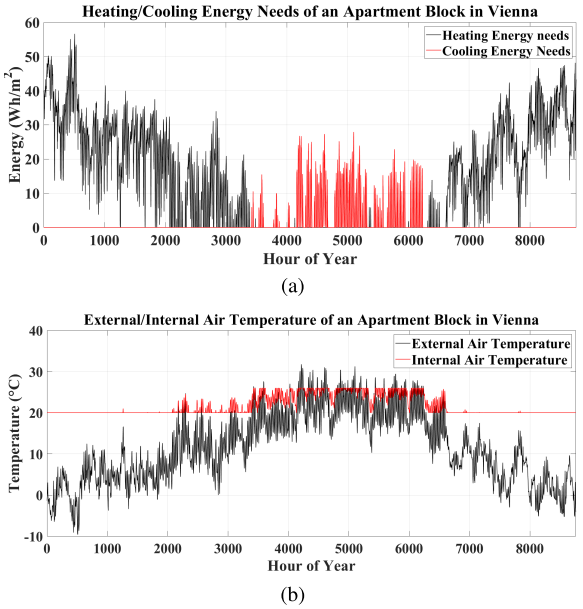

FIGURE 8. For a multi-apartment block in Vienna: (a) the hourly heating and cooling energy needs, and (b) the hourly internal and external air temperatures.

B. MULTI-APARTMENT BLOCK

In case of the multi-apartment block, the heating and cooling energy needs are clearly discriminated, as illustrated in Fig. 8. In the same manner to the single-family house, the heating energy needs present a gradual increase from September to December with several local drops in November, December and January. However, the peak value of heating demand is about 10 W/m^2 lower than the single-family house with a local peak of about 35 W/m^2 at the end of March. On the contrary, the cooling energy needs show a non-uniform distribution from May to August with the highest values in June and July, and peak value of less than 30 W/m^2.

Similarly to the single-family house, the internal air temperature of the examined multi-apartment block remains inside the range [20°C 26°C]. The multi-apartment block is also considered as a single zone, therefore, it is assumed that the total building is heated or cooled even when the occupancy is almost zero. Consequently, the calculated thermal energy needs are expected to be higher than the real ones, though there are time intervals during the year when no space heating and cooling are required, similarly to the case of single-family house. In practice, the occupancy of multi-apartment dwellings shall be computed for the occupants of each apartment, nevertheless, the variability of occupants' habits might burden the determination of multiple occupancy profiles. This was the main reason why in this study the same occupancy profile was used for both types of buildings.

The results of the proposed model on annual basis are compared with the results from other simulation tools in Table 5. As for the heating energy needs, the results of ISO 52016-01 have slighter deviations with EnergyPlus and EN13790 in comparison to INVERT/EE-Lab outcomes. On other hand, deviations of cooling energy needs vary from location to location, however, the differences are considerably shorter compared to the single-family house. In addition, in case of the building located in Seville, the annual cooling energy needs are higher than the annual heating energy needs due to the high temperature profile of the external air. Concerning the other locations, the annual heating demand significantly

TABLE 5. Summary of annual heating and cooling energy needs for the multi-apartment block.

Method [1]	Annual Heating Energy Needs (kWh/m^2)				Annual Cooling Energy Needs (kWh/m^2)			
	A	B	C	D	A	B	C	D
Seville	22.500	23.924	23.262	39.991	39.800	40.378	45.296	42.995
Madrid	64.700	80.347	76.940	101.440	23.200	20.442	22.855	28.749
Rome	40.300	46.619	43.026	37.553	24.700	17.210	18.251	18.077
Milan	99.900	116.850	111.740	99.882	15.900	9.0756	9.0756	19.974
Bucharest	118.900	95.815	104.130	113.680	20.600	52.925	31.951	20.670
Vienna	131.000	120.250	119.490	120.070	7.4000	8.3368	9.0947	10.137
Paris	146.000	158.670	161.510	145.500	3.0000	0.8900	3.1546	3.1444
Prague	117.900	121.010	120.510	114.530	3.6000	3.3000	4.5665	5.0731
Berlin	136.800	125.310	123.790	134.250	6.4000	3.5368	4.5474	3.0616
Helsinki	137.10	135.95	138.49	116.630	0.8000	2.5474	2.8039	0.2712

[1] **A: EnergyPlus, B: EN13790, C:INVERT/EE-Lab, D: ISO52016-1**

outweigh the annual cooling demand. In the same manner to the single-family house, the building located in Helsinki has the lowest heating energy needs due to lowest U-values of walls, roof and basement. In addition, the multi-apartment block located in Paris has the highest heating energy needs due to the highest U-values of the bulding elements.

Fig. 9 illustrates the monthly heating and cooling energy needs of a multi-apartment building located in the examined cities. It is evident that the outcomes related to heating demand have slighter deviations among the simulation tools compared to the outcomes for the single-family house. In addition, the highest differences were noticed for the multi-apartment dwelling located in Seville. As for the peak value of heating demand, the buildings in Bucharest and Paris have the highest values of about 35 W/m^2. In terms of cooling demand, shorter variations among the simulation tools were also observed compared to the single-family house. Besides that, the results of ISO 52016-01 for the buildings in Seville, Madrid, Rome, Milan and Vienna have the shorthest deviations with the other simulation tools. When applying the proposed model, the highest peak value of cooling demand was around 12 W/m^2 for the building in Seville, while the lowest peak value was 0.2 W/m^2 for the block in Helsinki.

C. DISCUSSION AND FUTURE WORK

Due to the different computation, the different level of building complexity, and the utilization description in the four simulation models, the thermal energy needs vary. Furthermore, any deviations on the results can also be influenced by different climate data that might have been used in the first three models. Particularly, any differences of ISO 52016 with EN 13790 can be due to the fact that a typical day per month was selected for the latter tool, while hourly data for each day of the simulated year were used for the former method. Concerning the g-values, EnergyPlus and EN 13790 models compute dynamic g-values, while both INVERT/EE-Lab and ISO 52016-01 models define constant values for each building.

Regarding the ventilation mechanism, the outcomes from EnergyPlus are derived using a complex ventilation control, which dynamically varies the ventilation rate with respect to indoor air condition and number of occupants per square meter. Besides that, variable ventilation rates were defined for different usage types of rooms (e.g. aisles, stairways, baths). In EN 13790 model, the ventilation rate can be hourly specified for the entire building, while the INVERT/EE-Lab approach specifies the ventilation rate between day and night times, non-using hours or using days and non-using days. On the contrary, a consistent ventilation rate of 0.5 l/s per m^2 was considered for the proposed model at summer nights. In addition, shading effects were only included by the other simulation programs.

As for the operative temperature, the proposed model considers both the internal air temperature and the internal surface temperature of all the building components. On the other hand, EnergyPlus and EN 13790 use the air temperature as operative temperature. As for the INVERT/EE-Lab model, the operative temperature was defined as follows:

$$\theta_{oper,t} = 0.3 \cdot \theta_{air,t} + 0.7 \cdot \theta_{s,t} \tag{19}$$

where $\theta_{s,t}$ is a combination of the air temperature and the mean radiant temperarure weighted by the internal surface convective and radiative coefficient. In addition, the monthly quasi-steady-state approach used in INVERT/EE-Lab model is not applicable in an hourly basis. It is also evident from the results that the INVERT/EE-Lab model leads to higher thermal energy needs compared to ISO 52016-01 model.

From the above discussion, it is concluded that the proposed model can approximate more accurately the operative temperature, since it takes into account the air temperature, as well as the temperatures and the areas of the internal surfaces. Using the EN ISO 52016-01 approach, the more complex operative temperature is applied as set temperature and it might also have impact on variations of the results. This simplified modelling considers the properties of the different property elements separately, unlike other modelling strategies that take into consideration an overall U-value of the property. Besides that, the opaque property elements are modelled according to their mass distribution, which improves the accuracy of the model. These two reasons make this way of modelling very adequate when analysing an existing property and the possible addition of insulation. Moreover, the hourly timestep considers several aspects that other simplified modelling does not take into account or does not model in a reliable manner, such as solar heat gains or thermal inertia. The computational time for the calculation

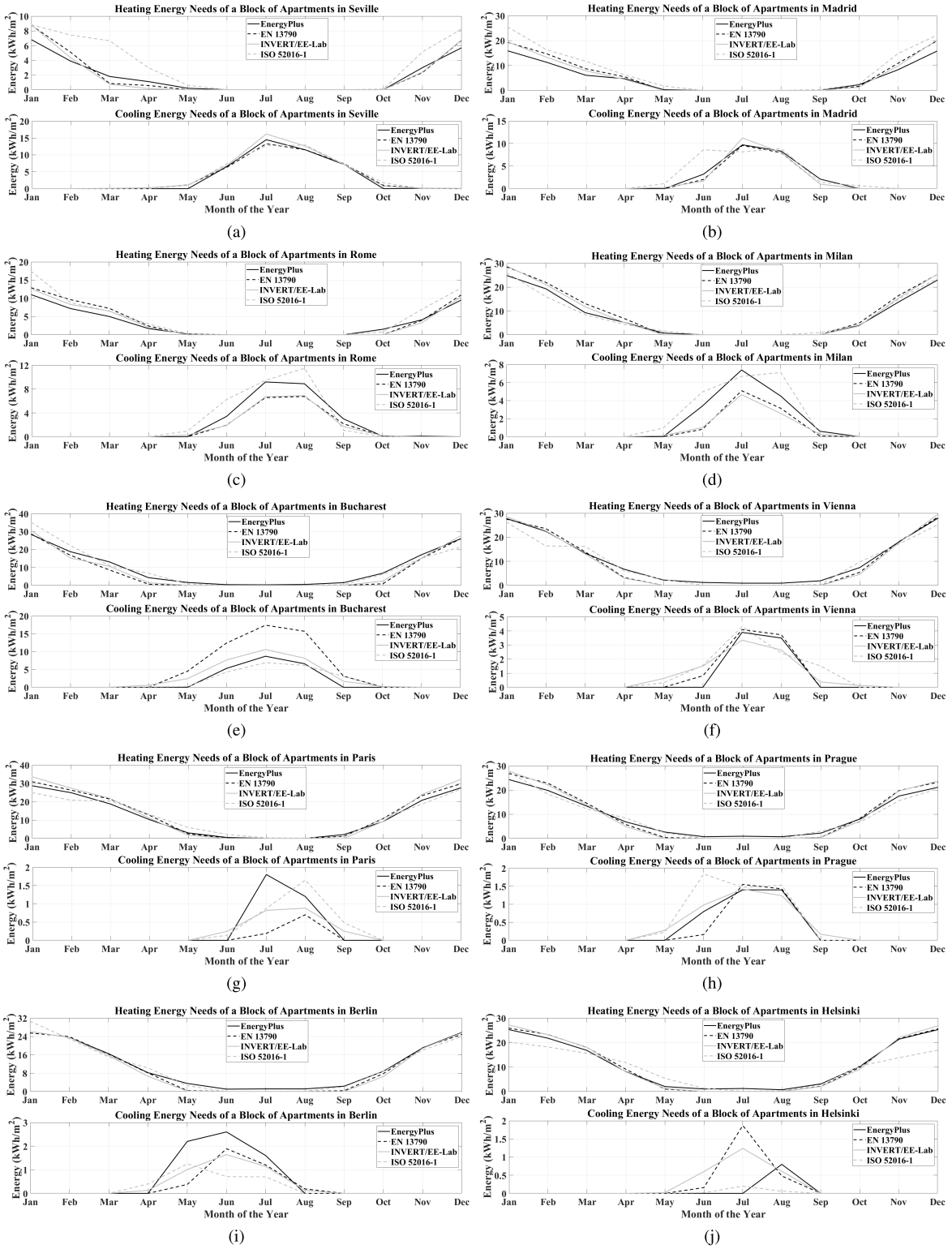

FIGURE 9. Monthly Thermal Energy Needs of a Multi-apartment Block in: (a) Seville, (b) Madrid, (c) Rome, (d) Milan, (e) Bucharest, (f) Vienna, (g) Paris, (h) Prague, (i) Berlin, (j) and Helsinki.

of heating and cooling needs throughout the year for one property, once the property data are imported, is less than 20 seconds. The simulations were carried out by a 64-bit system processor with CPU 2.3-2.4 GHz and RAM of 8 GB.

Due to the simplifications made in the energy model, there is a series of limitations that need to be considered before using the model. The model does not consider the effect of thermally unconditioned areas within the property. However,

if this is applied, the complexity would considerably increase, since the model should be especially designed for each specific property. One of the aspects that has not been taken into account is the effect of thermal bridges, thus, it would be interesting to study further.

Although the buildings examined are not located in any of the participant countries of the project PV-ESTIA, the proposed method can also be applied for any type of premises located in these countries. Ref. [61] provides examples of Greek premises located in different climatic zones for different insulation thickness of the walls. For an average insulation thickness of 4 cm, the annual heating energy needs range from 25 kWh/m^2 in Crete to 150 kWh/m^2 in Florina. On the other hand, the annual cooling energy needs present a respective range from 15 kWh/m^2 in Florina to about 50 kWh/m^2 in Athens. By comparing the aforementioned data with the outcomes of Tables 4 and 5, it is evident that the thermal energy needs in Greek premises can show high variabilities with respect to their location. In addition, the thermal energy demand in Greek buildings can approximate the respective values of buildings located in cities with warm climate such as Seville and Rome, as well as cities with continental climate, e.g. Bucharest, Prague and Vienna. In [62], the thermal energy needs for Cypriot residential buildings are assessed. For a single-family house constructed after 2006, the annual heating and cooling needs are about 36 kWh/m^2 and 50 kWh/m^2, respectively. In this case, the thermal needs approach to large extent the outcomes for the single-family house located in Seville due to the similarities in climatic conditions.

In terms of future work, the proposed thermal model is going to be combined with a stochastic technique for the calculation of the electrical energy consumption profile. Next, both thermal and electrical energy demand profiles can be used for the calculation of the optimal PV-storage system for various types of buildings, as well as to achieve optimal energy management with the proposed reinforcement solution.

VI. CONCLUSION

In this paper, a new method based on ISO 52016-01:2017 is proposed for the calculation of hourly heating and cooling energy needs in different types of buildings. The approach is considered as grey-box, since it combines physical-based formulations of the building envelope and measured data of various building parameters related to the architecture, material and weather-related data. The model computes the internal operative temperature on hourly basis for the whole year considering the external air temperature and the energy balance equations of the building components. Regarding the thermal energy calculation algorithm, space heating or cooling is required when the internal operative temperature cannot remain inside a temperature range predefined by the heating and cooling setpoints.

The proposed methodology was assessed for two different types of buildings, a single-family house and a multi-apartment block, which are located in ten European cities with climatic variations. The results from the simulations of the model were compared with the outcomes of other simulation tools (EnergyPlus, EN 13790 and INVERT/EE-Lab) used in the European project, ENTRANZE. From the assessment, it was clear that there were shorter deviations of ISO 52016-01 with the other simulation tools for the

TABLE 6. Usage factors for one-, two- and multi-dwelling buildings, by hour and day of the week.

h	Occupants		Appliances
	Weekdays	Weekends	(All Week)
1-6	1	1	0.5
7	0.5	0.8	0.5
8	0.5	0.8	0.7
9	0.5	0.8	0.7
10	0.1	0.8	0.5
11	0.1	0.8	0.5
12	0.1	0.8	0.6
13	0.1	0.8	0.6
14	0.2	0.8	0.6
15	0.2	0.8	0.6
16	0.2	0.8	0.5
17	0.5	0.8	0.5
18	0.5	0.8	0.7
19	0.5	0.8	0.7
20	0.8	0.8	0.8
21	0.8	0.8	0.8
22	0.8	0.8	0.8
23	1	1	0.6
24	1	1	0.6

TABLE 7. Fixed characteristics of the single-family house.

Building Geometry	
Number of heated floors	2
Surface/Volume	0.7 m^2/ m^3
Orientation	South/North
Net dimensions of heated volume	8.5 m x 8.5 m x 6.4 m
Net floor area of heated zones	144.5 m^2
Window area of south facade	25%
Window area of east facade	7%
Window area of north facade	25%
Window area of west facade	7%
Internal Gains	
Number of persons	3
Watts per person	102.6 W
Watts for lighting	3.5 W/m^2
Watts for appliances	4 W/m^2

TABLE 8. Fixed characteristics of the multi-apartment block.

Building Geometry	ES, IT, FR	RO, AT, CZ, DE, FI
Number of heated floors	4	
Surface/Volume	0.33 m^2/ m^3	
Orientation	South/North	
Net dimensions of heated volume	24.6 x 11.2 x 12.8 m	
Net floor area of heated zones	990 m^2	
Window area of south facade	15%	30%
Window area of east facade	0%	0%
Window area of north facade	15%	30%
Window area of west facade	0%	0%
Internal Gains		
Number of persons	25 m^2/person	
Watts per person	102.6 W	
Watts for lighting	3.5 W/m^2	
Watts for appliances	4 W/m^2	

TABLE 9. Variable characteristics of the single-family house.

Building Geometry	ES	IT	RO	AT	FR	CZ	DE	FI
Construction materials[1]	A	A	A	A	A	A	A	B
U-values of walls (W/m^{2}K)	1.46	1.21	1.45	1.25	1.54	1.32	0.93	0.48
U-values of roof (W/m^{2}K)	1.92	1.69	1.60	1.39	1.20	1.32	1.10	0.30
U-values of basement (W/m^{2}K)	1.30	1.69	1.30	1.77	1.97	1.24	1.01	0.48
U-values of glazings (W/m^{2}K)	5.70	3.20	2.40	2.70	4.20	2.90	2.57	2.79
g-values of glazings	0.89	0.80	0.75	0.75	0.80	0.75	0.75	0.75

[1] A: brick, concrete and plaster, and B: brick, insulation, concrete and plaster

TABLE 10. Variable characteristics of the multi-apartment block.

Building Geometry	ES	IT	RO	AT	FR	CZ	DE	FI
Construction materials[1]	A	A	C	B	B	B	B	B
U-values of walls (W/m^{2}K)	1.46	1.21	1.45	1.25	2.86	0.65	1.44	0.60
U-values of roof (W/m^{2}K)	1.92	1.69	1.20	1.39	2.56	0.65	1.17	0.39
U-values of basement (W/m^{2}K)	1.30	1.69	1.30	1.77	1.98	1.26	1.50	0.47
U-values of glazings (W/m^{2}K)	5.70	3.30	2.40	2.70	3.80	2.90	2.11	2.79
g-values of glazings	0.89	0.80	0.75	0.75	0.80	0.75	0.75	0.75

[1] A: Hollow brick, air gap, concrete, plaster, B: Concrete, plaster, C: Prefabricated panel, concrete, plaster

multi-apartment building. It was concluded that any differences are to due to differences in the internal air temperature, weather data, as well as the approaches of ventilation and shading effects, The proposed methodology can approximate more accurately the operative temperature, since it takes into account the air temperature, as well as the temperatures and the areas of the internal surfaces. Besides that, this simplified modelling considers the properties of all building components separately, while other modelling strategies take into account an overall U-value of the property. Finally, the short computational time for the calculation of heating and cooling needs throughout the year is one of the main advantages for the massive application of the proposed method.

APPENDIXES

APPENDIX A

The following factors are extracted from ISO 17772-1:2017 [55] (see Table 6).

APPENDIX B

The following tables provide the fixed and variable characteristics of the investigated buildings (see Tables 7–10).

REFERENCES

[1] United Nations Environment and International Energy Agency. (2017). *Global Status Report 2017: Towards a Zero-Emission, Efficient, and Resilient Buildings and Construction Sector*. [Online]. Available: https://www.worldgbc.org/.

[2] Energy Information Administration. *International Energy Outlook 2016—World Energy Demand and Economc Outlook*. Accessed: May 2016. [Online]. Available: https://www.eia.gov/outlooks/ieo/pdf/0484(2016).pdf

[3] European Commission. *EU Reference Scenario 2016: Energy, Transport and GHG Emissions—Trends to 2050*. Accessed: Jul. 20, 2016. [Online]. Available: https://ec.europa.eu/energy/

[4] European Commission, "Directive (EU) 2009/125/EC of the European parliament and of the council of 21 October 2009 establishing a framework for the setting of ecodesign requirements for energy-related products," *Off. J. Eur. Union*, vol. 285, pp. 10–35, Oct. 2009. Accessed: Oct. 2009. [Online]. Available: https://eur-lex.europa.eu/

[5] European Commission, "Regulation (EU) 2017/1369 of the European parliament and of the council of 4 July 2017 setting a framework for energy labelling and repealing directive 2010/30/EU," *Off. J. Eur. Union*, vol. 198, pp. 1–23, Jul. 2017. [Online]. Available: https://eur-lex.europa.eu/

[6] European Commission, "Directive 2002/91/EC of the European parliament and of the council of 16 December 2002 on the energy performance of buildings," *Off. J. Eur. Commun.*, vol. 1, pp. 65–71, Jan. 2003. [Online]. Available: https://eur-lex.europa.eu/

[7] European Commission, "Directive 2012/27/EU of the European parliament and of the council of 25 October 2012 on energy efficiency, amending directives 2009/125/EC and 2010/30/EU and repealing directives 2004/8/EC and 2006/32/EC," *Off. J. Eur. Union*, vol. 315, pp. 1–65, Nov. 2012. [Online]. Available: https://eur-lex.europa.eu/

[8] M. Economidou and P. Bertoldi, "Assessment of the national energy efficiency action plans 2017 under the energy efficiency directive," in *Proc. Inter. Ener. Pol. Prog. Eval. Conf.*, Vienna, Austria, 2018, pp. 1–12.

[9] European Commission, "Directive (EU) 2018/844 of the European parliament and of the council of 30 May on the energy performance of buildings and directive 2012/27/EU on energy efficiency," *Off. J. Eur. Union*, vol. 156, pp. 75–91, Jun. 2018. [Online]. Available: https://eur-lex.europa.eu/

[10] European Commission, "Directive 2010/31/EU of the European parliament and of the council of 19 May 2010 on the energy performance of buildings (recast)," *Off. J. Eur. Union*, vol. 153, pp. 13–53, Jun. 2010. [Online]. Available: https://eur-lex.europa.eu/

[11] Y. Han, X. Liu, and L. Chang, "Comparison of software for building energy simulation," *J. Chem. Pharm. Res.*, vol. 6, no. 3, pp. 471–476, Jan. 2014.

[12] EnergyPlus 9.0.2. Department of Energy's. Building Technologies Office. USA. [Online]. Available: https://energyplus.net/

[13] ESP-r. Department of Mechanical Engineering. University of Strathclyde. Glasgow, U.K. [Online]. Available: http://www.esru.strath.ac.uk/Programs/ESP-r.htm

[14] DOE-2. Building Energy Use and Cost Analysis Software. JJH. San Diego, CA, USA. [Online]. Available: http://www.doe2.com/

[15] TRNSYS. Transient System Simulation Program. University of Wisconsin. Accessed: 2000. [Onilne]. Available: http://www.trnsys.com/

[16] B. Delcroix, "Modeling of thermal mass energy storage in buildings with phase change materials," Ph.D. dissertation, Univ. Montreal, Montreal, QC, Canada, 2015.

[17] M. Deru, R. Judkoff, and J. Neymark, "Whole-building energy simulation with a three dimensional ground-coupled heat transfer model," in *Proc. Winter Meet. Amer. Soc. Heat., Refrig. Air-Cond. Engin., Inc. (ASHRAE)*, Chicago, IL, USA, 2003, pp. 1–18.

[18] L. Mei, D. Infield, U. Eicker, and V. Fux, "Thermal modelling of a building with an integrated ventilated PV façade," *Energy Buildings*, vol. 35, no. 6, pp. 605–617, Jul. 2003, doi: 10.1016/S0378-7788(02)00168-8.

[19] C. Koo, S. Park, T. Hong, and H. S. Park, "An estimation model for the heating and cooling demand of a residential building with a different envelope design using the finite element method," *Appl. Energy*, vol. 115, pp. 205–215, Feb. 2014, doi: 10.1016/j.apenergy.2013.11.014.

[20] A. Fateh, D. Borelli, A. Spoladore, and F. Devia, "A state-space analysis of a single zone building considering solar radiation, internal radiation, and PCM effects," *Appl. Sci.*, vol. 9, no. 5, p. 832, Feb. 2019, doi: 10.3390/app9050832.

[21] C. Yan, S. Wang, K. Shan, and Y. Lu, "A simplified analytical model to evaluate the impact of radiant heat on building cooling load," *Appl. Thermal Eng.*, vol. 77, pp. 30–41, Feb. 2015, doi: 10.1016/j.applthermaleng.2014.12.017.

[22] T. R. Nielsen, "Simple tool to evaluate energy demand and indoor environment in the early stages of building design," *Solar Energy*, vol. 78, no. 1, pp. 73–83, Jan. 2005, doi: 10.1016/j.solener.2004.06.016.

[23] M. De Rosa, M. Brennenstuhl, C. Andrade Cabrera, U. Eicker, and D. P. Finn, "An iterative methodology for model complexity reduction in residential building simulation," *Energies*, vol. 12, no. 12, p. 2448, Jun. 2019, doi: 10.3390/en12122448.

[24] C. S. Barnaby and J. D. Spitler, "Development of the residential load factor method for heating and cooling load calculations," *ASHRAE Trans.*, vol. 111, pp. 291–307, Jan. 2005.

[25] Z. Romani, A. Draoui, and F. Allard, "Metamodeling the heating and cooling energy needs and simultaneous building envelope optimization for low energy building design in Morocco," *Energy Buildings*, vol. 102, pp. 139–148, Sep. 2015, doi: 10.1016/j.enbuild.2015.04.014.

[26] J. S. Hygh, J. F. Decarolis, D. B. Hill, and S. Ranji Ranjithan, "Multivariate regression as an energy assessment tool in early building design," *Building Environ.*, vol. 57, pp. 165–175, Nov. 2012, doi: 10.1016/j.buildenv.2012.04.021.

[27] I. Korolija, Y. Zhang, L. Marjanovic-Halburd, and V. I. Hanby, "Regression models for predicting UK office building energy consumption from heating and cooling demands," *Energy Buildings*, vol. 59, pp. 214–227, Apr. 2013, doi: 10.1016/j.enbuild.2012.12.005.

[28] S. Paudel, P. H. Nguyen, W. L. Kling, M. Elmitri, B. Lacarrière, and O. L. Corre, "Support vector machine in prediction of building energy demand using pseudo dynamic approach," in *Proc. ECOS*, Pau, France, 2015, pp. 1–14.

[29] E. T. Al-Shammari, A. Keivani, S. Shamshirband, A. Mostafaeipour, P. L. Yee, D. Petković, and S. Ch, "Prediction of heat load in district heating systems by support vector machine with firefly searching algorithm," *Energy*, vol. 95, pp. 266–273, Jan. 2016, doi: 10.1016/j.energy.2015.11.079.

[30] M. Protić, S. Shamshirband, D. Petković, A. Abbasi, M. L. Mat Kiah, J. A. Unar, L. Živković, and M. Raos, "Forecasting of consumers heat load in district heating systems using the support vector machine with a discrete wavelet transform algorithm," *Energy*, vol. 87, pp. 343–351, Jul. 2015, doi: 10.1016/j.energy.2015.04.109.

[31] Q. Li, Q. Meng, J. Cai, H. Yoshino, and A. Mochida, "Predicting hourly cooling load in the building: A comparison of support vector machine and different artificial neural networks," *Energy Convers. Manage.*, vol. 50, no. 1, pp. 90–96, Jan. 2009, doi: 10.1016/j.enconman.2008.08.033.

[32] J. W. Moon and J.-J. Kim, "ANN-based thermal control models for residential buildings," *Building Environ.*, vol. 45, no. 7, pp. 1612–1625, Jul. 2010, doi: 10.1016/j.buildenv.2010.01.009.

[33] R. Escandon, F. Ascione, N. Bianco, G. M. Mauro, R. Suárez, and J. J. Sendra, "Thermal comfort prediction in a building category: Artificial neural network generation from calibrated models for a social housing stock in southern Europe," *Appl. Thermal Eng.*, vol. 150, pp. 492–505, Mar. 2019, doi: 10.1016/j.applthermaleng.2019.01.013.

[34] L. Magnier and F. Haghighat, "Multiobjective optimization of building design using TRNSYS simulations, genetic algorithm, and artificial neural network," *Building Environ.*, vol. 45, no. 3, pp. 739–746, Mar. 2010, doi: 10.1016/j.buildenv.2009.08.016.

[35] S. Gou, V. M. Nik, J.-L. Scartezzini, Q. Zhao, and Z. Li, "Passive design optimization of newly-built residential buildings in Shanghai for improving indoor thermal comfort while reducing building energy demand," *Energy Buildings*, vol. 169, pp. 484–506, Jun. 2018, doi: 10.1016/j.enbuild.2017.09.095.

[36] O. T. Ogunsola, L. Song, and G. Wang, "Development and validation of a time-series model for real-time thermal load estimation," *Energy Buildings*, vol. 76, pp. 440–449, Jun. 2014, doi: 10.1016/j.enbuild.2014.02.075.

[37] P. Bacher and H. Madsen, "Identifying suitable models for the heat dynamics of buildings," *Energy Buildings*, vol. 43, no. 7, pp. 1511–1522, Jul. 2011, doi: 10.1016/j.enbuild.2011.02.005.

[38] S. Wang and X. Xu, "Parameter estimation of internal thermal mass of building dynamic models using genetic algorithm," *Energy Convers. Manage.*, vol. 47, nos. 13–14, pp. 1927–1941, Aug. 2006, doi: 10.1016/j.enconman.2005.09.011.

[39] A. Bagheri, V. Feldheim, D. Thomas, and C. S. Ioakimidis, "Coupling building thermal network and control system, the first step to smart buildings," in *Proc. IEEE Int. Smart Cities Conf. (ISC)*, Trento, Italy, Sep. 2016, pp. 1–6.

[40] B.-K. Jeon, E.-J. Kim, Y. Shin, and K.-H. Lee, "Learning-based predictive building energy model using weather forecasts for optimal control of domestic energy systems," *Sustainability*, vol. 11, no. 1, p. 147, Dec. 2018, doi: 10.3390/su11010147.

[41] G. Fraisse, C. Viardot, O. Lafabrie, and G. Achard, "Development of a simplified and accurate building model based on electrical analogy," *Energy Buildings*, vol. 34, no. 10, pp. 1017–1031, Nov. 2002, doi: 10.1016/s0378-7788(02)00019-1.

[42] A. Tindale, "Third-order lumped-parameter simulation method," *Building Services Eng. Res. Technol.*, vol. 14, no. 3, pp. 87–97, Aug. 1993, doi: 10.1177/014362449301400302.

[43] S. Wang and X. Xu, "Simplified building model for transient thermal performance estimation using GA-based parameter identification," *Int. J. Thermal Sciences*, vol. 45, no. 4, pp. 419–432, Apr. 2006, doi: 10.1016/j.ijthermalsci.2005.06.009.

[44] Q. Zhou, S. Wang, X. Xu, and F. Xiao, "A grey-box model of next-day building thermal load prediction for energy-efficient control," *Int. J. Energy Res.*, vol. 32, no. 15, pp. 1418–1431, Dec. 2008, doi: 10.1002/er.1458.

[45] M. De Rosa, V. Bianco, F. Scarpa, and L. A. Tagliafico, "Heating and cooling building energy demand evaluation; a simplified model and a modified degree days approach," *Appl. Energy*, vol. 128, pp. 217–229, Sep. 2014, doi: 10.1016/j.apenergy.2014.04.067.

[46] G. Capizzi, G. L. Sciuto, G. Cammarata, and M. Cammarata, "Thermal transients simulations of a building by a dynamic model based on thermal-electrical analogy: Evaluation and implementation issue," *Appl. Energy*, vol. 199, pp. 323–334, Aug. 2017, doi: 10.1016/j.apenergy.2017.05.052.

[47] E. Monstvilas, V. Stankevičius, J. Karbauskaité, A. Burlingis, and K. Banionis, "Hourly calculation method of building energy demand for space heating and cooling based on steady-state heat balance equations," *J. Civil Eng. Manage.*, vol. 18, no. 3, pp. 356–368, Jun. 2012, doi: 10.3846/13923730.2012.689994.

[48] E. Elsarrag and Y. Alhorr, "Modelling the thermal energy demand of a passive-house in the gulf region: The impact of thermal insulation," *Int. J. Sustain. Built Environ.*, vol. 1, no. 1, pp. 1–15, Jun. 2012, doi: 10.1016/j.ijsbe.2012.07.002.

[49] P. Zangheri, R. Armani, M. Pietrobon, L. Pagliano, M. F. Boneta, and A. Müller, "Heating and cooling energy demand and loads for building types in different countries of the EU," Inst. Energy Syst. Elect. Drives, Vienna, Austria, D2.3. of WP2 of the Entranze Project, Mar. 2014.

[50] R. Bruno, P. Bevilacqua, and N. Arcuri, "Assessing cooling energy demands with the EN ISO 52016-1 quasi-steady approach in the Mediterranean area," *J. Building Eng.*, vol. 24, Jul. 2019, Art. no. 100740, doi: 10.1016/j.jobe.2019.100740.

[51] T. Zakula, M. Bagaric, N. Ferdelji, B. Milovanovic, S. Mudrinic, and K. Ritosa, "Comparison of dynamic simulations and the ISO 52016 standard for the assessment of building energy performance," *Appl. Energy*, vol. 254, Nov. 2019, Art. no. 113553, doi: 10.1016/j.apenergy.2019.113553.

[52] N. Efkarpidis, G. Christoforidis, and G. Papagiannis, "Modelling of thermal energy demand in smart buildings," in *Proc. IEEE Int. Conf. Environment Electr. Eng., IEEE Ind. Commercial Power Syst. Europe (EEEIC/I CPS Eur.)*, Genova, Italy, Jun. 2019, pp. 1–6.

[53] *Energy Performance of Buildings—Energy Needs for Heating and Cooling, Internal Temperatures and Sensible and Latent Heat Loads—Part 1: Calculation Procedures*. Standard ISO, 52016-1:2017, ISO/TC 163/SC 2 Calculation Methods, 2017.

[54] T. Bauer, W.-D. Steinmann, D. Laing, and R. Tamme, "Thermal energy storage materials and systems," *Annu. Rev. Heat Transf.*, vol. 15, pp. 131–177, Jan. 2012, doi: 10.1615/AnnualRevHeatTransfer.2012004651.

[55] *Energy Performance of Buildings—Indoor Environmental Quality Part 1: Indoor Environmental Input Parameters for the Design and Assessment of Energy Performance of Buildings*. Standard ISO, 17772-1:2017, ISO/TC 163 Thermal Performance and Energy Use in the Built Environment, 2017.

[56] *ASHRAE Handbook—Fundamentals (SI Edition)*, Amer. Soc. Heating, Refrigerating Air-Conditioning Eng., Atlanta, GA, USA, 2001.

[57] *Thermal Performance of Buildings—Heat Transfer Via the Ground Calculation Methods*. Standard ISO, 13370:2017, ISO/TC 163/SC 2 Calculation Methods, 2017.

[58] *Thermal Performance of Buildings—Transmission and Ventilation Heat Transfer Coefficients—Calculation Method*, Standard ISO, 13789:2017, ISO/TC 163/SC 2 Calculation Methods, 2017.
[59] *Building Components and Building Elements—Thermal Resistance and Thermal Transmittance—Calculation Methods*, Standard ISO, 6946:2017, ISO/TC 163/SC 2 Calculation Methods, 2017.
[60] *PV-GIS, Solar Radiation Database*. [Online]. Available: https://re.jrc.ec.europa.eu/
[61] G. Mitsopoulos, E. Bellos, and C. Tzivanidis, "Financial and energetic optimization of Greek buildings insulation," *Designs*, vol. 2, no. 3, p. 34, Sep. 2018, doi: 10.3390/designs2030034.
[62] M. Economidou, P. Zangheri, A. Müller, and L. Kranzl, "Financing the renovation of the cypriot building stock: An assessment of the energy saving potential of different policy scenarios based on the invert/EE-Lab model," *Energies*, vol. 11, no. 11, p. 3071, Nov. 2018, doi: 10.3390/en11113071.

NIKOLAOS A. EFKARPIDIS received the master's degree from the Department of Electrical and Computer Engineering, Aristotle University of Thessaloniki (AUTH), Greece, in 2010, and the Ph.D. degree in electrical engineering from the Group of ESAT, KU Leuven, Belgium, in 2016. He is currently working as a Research Associate with the Institute of Power Systems, University of Applied Sciences and Arts Northwestern Switzerland (FHNW), Switzerland. His main fields of interests include the power quality control in power systems, development of optimization algorithms at both networks, and end-user level, as well as design and operation of nZEBs.

GEORGIOS C. CHRISTOFORIDIS (Senior Member, IEEE) received the Dipl.Eng. degree from the Electrical Engineering Department, AUTH, in 1998, the M.Sc. degree (Hons.) in power electronics and drives from the Electrical and Electronic Engineering Department, University of Birmingham, U.K., in 1999, and the Ph.D. degree from AUTH, in 2004. Since 2019, he has been with the Electrical and Computer Engineering Department, University of Western Macedonia, Kozani, Greece, as a Professor of power systems. His main research interests include distribution power networks, smart grids, integration of renewable energy sources, and EMC. He has authored or coauthored 94 articles in these fields.

GRIGORIS K. PAPAGIANNIS (Senior Member, IEEE) received the Dipl.Eng. and Ph.D. degrees from the School of Electrical and Computer Engineering, Aristotle University of Thessaloniki, in 1979 and 1998, respectively. He is currently a Professor of power systems analysis and the Head of the School of Electrical and Computer Engineering. His research interests are power systems modeling, computation of electromagnetic transients, distributed generation, power-line communications, and smart grids. He is the author or coauthor of 167 articles on these fields.